DOI: 10.1002/ejic.201101026

Ruthenium(III) Cyclometalates Obtained by Site-Specific Orthometallation and Their Reactivity with Nitric Oxide: Photoinduced Release and Estimation of NO Liberated from the Ruthenium Nitrosyl Complexes

Kaushik Ghosh,*[a] Sushil Kumar,[a] Rajan Kumar,[a] and Udai P. Singh[a]

Keywords: Ruthenium / Redox chemistry / Metalation / Photolability

Cyclometalated Ru^{III} complexes $[Ru(L^{SB1})(PPh_3)_2Cl]$ (**1**), [$L^{SB1}H_2$ = 2-(3-nitrobenzylideneamino)phenol], and $[Ru(L^{SB2})(PPh_3)_2Cl]$ (**2**), [$L^{SB2}H_2$ = 4-methyl-2-(3-nitrobenzylideneamino)phenol and H = dissociable protons], were synthesized by site-specific orthometallation and characterized by spectroscopic and electrochemical studies. Complexes **1** and **2** were treated with in situ generated nitric oxide (NO), derived from an acidified nitrite solution, which afforded the ruthenium nitrosyl complexes $[Ru(L^{SB3}H)(PPh_3)_2(NO)Cl](ClO_4)$ (**1a**) and $[Ru(L^{BOX})(PPh_3)_2(NO)Cl](ClO_4)$ (**2a**), respectively, [$L^{SB3}H_2$ = 4-nitro-2-(3-nitrobenzylideneamino)-phenol, $L^{BOX}H$ = 5-methyl-7-nitro-2-(3-nitrophenyl)benzoxazole and H = dissociable protons]. Complexes **1a** and **2a** were found to be diamagnetic and were characterized by ^1H NMR and ^{31}P NMR spectral studies. Both **1a** and **2a** exhibited ν_{NO} in the range 1800–1835 cm^{-1} in the IR spectra. Molecular structures of σ-aryl ruthenium nitrosyl complexes **1a**·CH_3OH·$2CH_2Cl_2$·H_2O and **2a**·$2CH_2Cl_2$ were determined by X-ray crystallography. Nitrosylation at the metal centre, oxidative cyclization and ligand nitration were authenticated from the crystal structures. The redox properties of the metal centre were investigated. In both the nitrosyl complexes **1a** and **2a**, coordinated NO was found to be photolabile. The amount of photoreleased NO was estimated by using the Griess reagent and the data was compared with that obtained from sodium nitroprusside (SNP). The role of the nitro group in the ligand frame was discussed with regard to orthometallation, NO reactivity and photolability.

Introduction

Organometallic ruthenium cyclometalates incorporating trivalent ruthenium are scarce.[1–6] An investigation of the literature of trivalent ruthenium organometallic complexes revealed that the complexes are formed through C–H activation and the concomitant formation of a σ-aryl ruthenium–carbon bond. It has been found that in the case of ruthenium(III) cyclometalates derived from Schiff-base ligands, the metal–carbon bond is established through orthometallation with the phenyl ring that has an aldehyde functional group, see Scheme 1 (A), X = CH, Type 1.[3] On the other hand, there is another group of structurally similar complexes where instead of azomethine nitrogen, the azo function is bound to the Ru^{III} centre. In these types of complexes, orthometallation is observed with the ring that has been contributed by the aromatic amine during the azo coupling reaction, as shown in Scheme 1 (A), X = N, Type 2.[4,6] In both cases either *para*-substituted benzaldehyde, during Schiff-base formation, or *para*-substituted aromatic amines were used during the ligand synthesis. Hence, for the synthesis of the ruthenium complexes, a single site for orthometallation was found to be available in both the type 1 and type 2 ligands. To the best of our knowledge, there is no report in the literature where a type 1 or type 2 ligand was used to provide more than one site for the metal centre to establish a ruthenium–carbon bond during the synthesis of ruthenium cyclometalates. Hence, in this endeavour, we have chosen Schiff-base ligands derived from *m*-nitrobenzaldehyde and 2-aminophenol and substituted 2-aminophenol [shown in Scheme 1 (B)] to investigate the mode of σ-aryl ruthenium–carbon bond formation.

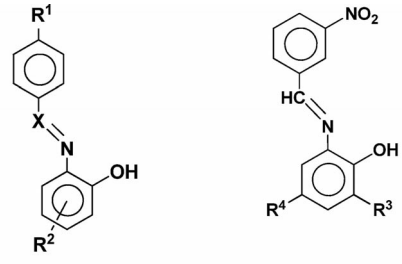

A B

Type 1 (X = CH)	Type 2 (X = N)	R^3	R^4	Ligand
R^1 = H, Cl, CH_3 or NO_2		H	H	$L^{SB1}H_2$
R^2 = H or CH_3		H	CH_3	$L^{SB2}H_2$
		H	NO_2	$L^{SB3}H_2$

Scheme 1.

[a] Department of Chemistry, Indian Institute of Technology, Roorkee, Roorkee 247667, Uttarakhand, India
Fax: +91-1332-273560
E-mail: ghoshfcy@iitr.ernet.in

Synthesis and characterization of ruthenium nitrosyl complexes and studies on the generation of nitric oxide (NO) on demand have recieved considerable attention.[7–9] An investigation of the literature revealed that there is no report on the reactivity of nitric oxide with ruthenium cyclometalates incorporating trivalent ruthenium. To the best of our knowledge, a single report by Crutchley and coworkers[5] is available in the literature, however, the nitrosyl complex was not utilized for the generation of NO. This work stems from our interest to synthesize novel ruthenium nitrosyl complexes derived from these ruthenium cyclometalates. In recent reports, we have described the role of *trans*-directing carbanion in the coordination and photolability of NO.[10,11] Moreover, we have observed the effect of substituents on the phenyl ring containing the phenolato function. In our previous reports, we always used *para*-substituted benzaldehydes for the synthesis of Schiff bases and the effect of the substituent on the phenyl ring containing the aldehyde function was not discussed. Hence, *meta*-substituted benzaldehyde has never been used for the synthesis of ruthenium cyclometalates (vide supra) as well as ruthenium nitrosyl complexes derived from those cyclometalates. Herein we report on the synthesis and characterization of ruthenium cyclometalates $[Ru(L^{SB1})(PPh_3)_2Cl]$ (**1**) [where $L^{SB1}H_2$ is 2-(3-nitrobenzylideneamino)phenol] and $[Ru(L^{SB2})(PPh_3)_2Cl]$ (**2**) [where $L^{SB2}H_2$ is 4-methyl-2-(3-nitrobenzylideneamino)phenol] [H is the dissociable proton, Scheme 1 (B)] derived from Schiff-base ligands $L^{SB1}H_2$ and $L^{SB2}H_2$, respectively, and their site-specific orthometallation (Scheme 2).

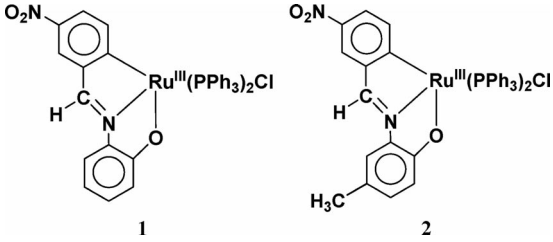

1 2

Scheme 2.

The interaction of NO with these organometallic ruthenium complexes was investigated and the resultant complexes $[Ru(L^{SB3}H)(PPh_3)_2(NO)Cl](ClO_4)$ (**1a**) and $[Ru(L^{BOX})(PPh_3)_2(NO)Cl](ClO_4)$ (**2a**) [$L^{SB3}H_2$ = 4-nitro-2-(3-nitrobenzylideneamino)phenol, $L^{BOX}H$ = 5-methyl-7-nitro-2-(3-nitrophenyl)benzoxazole and H = dissociable protons] were synthesized and characterized (Scheme 3).

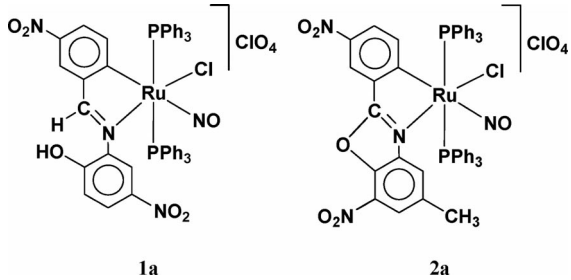

1a 2a

Scheme 3.

Molecular structures of **1a**·CH_3OH·$2CH_2Cl_2$·H_2O and **2a**·$2CH_2Cl_2$ were determined by X-ray crystallography. The redox properties of the metal centre in these complexes were investigated in order to better understand the stabilization of the ruthenium oxidation state after orthometallation. The photolability of coordinated NO was authenticated by UV/Vis spectral studies and liberated NO was trapped by reduced myoglobin. Photoreleased NO was not estimated in our previous reports,[10,11] however, in this report we estimated NO after photodissociation by a Griess reagent using visible as well as UV light. Sodium nitroprusside (SNP), which is utilized for the treatment of cardiovascular disorder and blood pressure regulation through the release of NO,[12–14] was used as the standard.

The role of the electron-withdrawing $–NO_2$ group on the phenyl ring, ligated to the metal centre through a σ-aryl bond, will be discussed in the context of light-induced delivery of nitric oxide.

Results and Discussion

Synthesis

The complexes $[Ru(L^{SB1})(PPh_3)_2Cl]$ (**1**) and $[Ru(L^{SB2})(PPh_3)_2Cl]$ (**2**) were synthesized by the reaction of $Ru(PPh_3)_3Cl_2$ with the Schiff base ligands $L^{SB1}H_2$ and $L^{SB2}H_2$, respectively, in ethanol.[3] Complexes **1** and **2** (Scheme 2) were red-brown in colour and both complexes were isolated in good yield. They were highly soluble in dichloromethane and benzene but were much less soluble in polar solvents like water and methanol. Dichloromethane solutions of **1** and **2** were treated with in situ generated NO derived from an acidified nitrite ($NaNO_2$) solution with continuous stirring for 2 h.[10] The red-brown colour of the solution disappeared and the formation of an orange-yellow colour was observed. A methanolic solution of $NaClO_4$ was added to provide ClO_4^- ions to stabilize the large cationic ruthenium nitrosyl complexes. $[Ru(L^{SB3}H)(PPh_3)_2(NO)Cl](ClO_4)$ (**1a**) and $[Ru(L^{BOX})(PPh_3)_2(NO)Cl](ClO_4)$ (**2a**) (Scheme 3) were derived from **1** and **2**, respectively. Both the nitrosyl complexes **1a** and **2a** were recrystallized from a dichloromethane/methanol mixture. Complexes **1a** and **2a** were highly soluble in organic solvents like dichloromethane, acetonitrile, dimethylformamide and methanol, however, lower solubility was observed in water.

Description of Structures

The molecular structures of complexes $[Ru(L^{SB3}H)(PPh_3)_2(NO)Cl](ClO_4)$·$CH_3OH$·$2CH_2Cl_2$·$H_2O$ (**1a**·CH_3OH·$2CH_2Cl_2$·H_2O) and $[Ru(L^{BOX})(PPh_3)_2(NO)Cl](ClO_4)$·$2CH_2Cl_2$ (**2a**·$2CH_2Cl_2$) are depicted in Figure 1 and Figure 2, respectively. The matrix parameters of these complexes are described in Table 4 and the selected bond lengths and bond angles are given in Table 1.

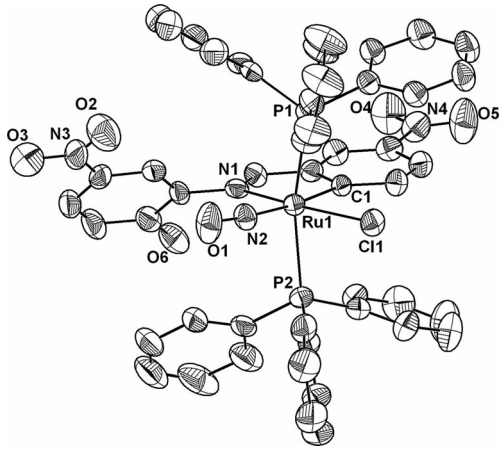

Figure 1. ORTEP diagram (50% probability level) of the cation of the complex $[Ru(L^{SB3}H)(PPh_3)_2(NO)Cl](ClO_4)\cdot CH_3OH\cdot 2CH_2Cl_2\cdot H_2O$ (**1a**·CH_3OH·$2CH_2Cl_2$·H_2O). All hydrogen atoms and solvent molecules are omitted for clarity.

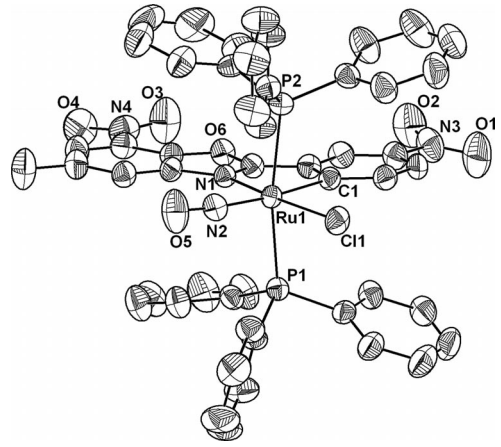

Figure 2. ORTEP diagram (50% probability level) of the cation of the complex $[Ru(L^{BOX})(PPh_3)_2(NO)Cl](ClO_4)\cdot 2CH_2Cl_2$ (**2a**·$2CH_2Cl_2$). All hydrogen atoms and solvent molecules are omitted for clarity.

In the molecular structure of **1a**·CH_3OH·$2CH_2Cl_2$·H_2O, carbanion (C1), Cl(1), NO and the imine nitrogen (N1) constitute the equatorial plane whereas the phosphane groups occupy the axial positions *trans* to each other. So, the geometry around the metal centre is found to be distorted octahedral. Interestingly, in **1a**·CH_3OH·$2CH_2Cl_2$·H_2O, the phenolato oxygen is not bound to the metal centre and protonation gave rise to a phenolic –OH function, which was consistent with our ^1H NMR spectroscopic data (vide infra). Hence, in this structure we observed that the tridentate ligand in the precursor complex **1** became bidentate in the σ-aryl ruthenium nitrosyl complex **1a**·CH_3OH·$2CH_2Cl_2$·H_2O. The tilting of the phenyl ring containing a phenolato function afforded a dihedral angle of ca. 47° with the ligand binding plane. Moreover, ligand nitration was observed on the phenyl ring containing the phenolato function and the site of nitration was *trans* to the phenolato function.

Table 1. Selected bond lengths and bond angles of complexes $[Ru(L^{SB3}H)(PPh_3)_2(NO)Cl](ClO_4)\cdot CH_3OH\cdot 2CH_2Cl_2\cdot H_2O$ (**1a**·CH_3OH·$2CH_2Cl_2$·H_2O) and $[Ru(L^{BOX})(PPh_3)_2(NO)Cl]ClO_4\cdot 2CH_2Cl_2$ (**2a**·$2CH_2Cl_2$).

Bond lengths [Å]		Bond angles [°]	
1a·CH_3OH·$2CH_2Cl_2$·H_2O			
Ru(1)–Cl(1)	2.3755(10)	N(2)–Ru(1)–C(1)	170.81(10)
Ru(1)–P(1)	2.4651(11)	N(2)–Ru(1)–Cl(1)	100.64(8)
Ru(1)–P(2)	2.4425(10)	C(1)–Ru(1)–Cl(1)	88.38(8)
Ru(1)–C(1)	2.100(2)	N(2)–Ru(1)–P(1)	93.76(7)
Ru(1)–N(2)	1.799(2)	N(1)–Ru(1)–P(1)	95.66(6)
Ru(1)–N(1)	2.137(2)	C(1)–Ru(1)–P(1)	85.07(7)
N(2)–O(1)	1.152(3)	P(1)–Ru(1)–P(2)	168.04(3)
		O(1)–N(2)–Ru(1)	170.90(2)
2a·$2CH_2Cl_2$			
Ru(1)–Cl(1)	2.3534(11)	N(1)–Ru(1)–C(1)	77.84(15)
Ru(1)–P(1)	2.4435(12)	N(2)–Ru(1)–Cl(1)	97.47(12)
Ru(1)–P(2)	2.4306(12)	C(1)–Ru(1)–Cl(1)	91.30(12)
Ru(1)–C(1)	2.108(4)	C(1)–Ru(1)–P(1)	86.63(12)
Ru(1)–N(1)	2.105(3)	Cl(1)–Ru(1)–P(2)	90.23(4)
Ru(1)–N(2)	1.786(4)	P(1)–Ru(1)–P(2)	169.78(4)
N(2)–O(5)	1.140(5)	O(5)–N(2)–Ru(1)	170.90(4)

The molecular structure of the nitrosyl complex **2a**·$2CH_2Cl_2$ is different from that of **1a**·CH_3OH·$2CH_2Cl_2$·H_2O in certain aspects. Similar to the previous structure, it has been found out that the phenolato function is not attached to the ruthenium centre and that the ligand is chelated in a bidentate fashion, however, in the case of **2a**·$2CH_2Cl_2$ oxidative cyclization[10] was observed.

The carbanion (C1) and imine nitrogen (N1) from the substituted 2-phenylbenzoxazole moiety along with the Cl^- and NO ligands constitute the equatorial plane whereas the two *trans*-PPh_3 groups are found at the axial positions. The P1–Ru1–P2, N1–Ru1–Cl1 and C1–Ru1–N2 angles indicate a distorted octahedral geometry around the metal centre. On the other hand in **2a**·$2CH_2Cl_2$ oxidative cyclization and benzoxazole formation was observed. Hence phenolato –OH is not present in the molecule and the ring with the phenolato function is found to be in the plane with the ligand. For this we did not find any –OH peak in the ^1H NMR spectrum. The presence of *trans*-PPh_3 groups in both the complexes is consistent with the ^{31}P NMR spectroscopic data (vide infra).[15,16]

In both the nitrosyl complexes, Ru–N_{NO} distances [1.799(2) Å in **1a**·CH_3OH·$2CH_2Cl_2$·H_2O and 1.786(4) Å in **2a**·$2CH_2Cl_2$] were found to be longer than those reported,[17–19] which may be due to the *trans* effect of carbanion (C1).[4,6] However, this value was close to the value reported by Crutchley and coworkers.[5] The N–O distance in both the complexes was found to be consistent with the values given in the literature.[16–18] All these data along with Ru–N–O angles (≈171°) in **1a**·CH_3OH·$2CH_2Cl_2$·H_2O and **2a**·$2CH_2Cl_2$ clearly show a $\{Ru^{II}–NO^+\}^6$ description[7] of the $\{Ru–NO\}^6$ moiety.[20] This is also supported by IR spectroscopic data described in the next section.

The noncovalent interactions are very important in supramolecular chemistry and crystal engineering.[21] The interactions found in **1a**·CH_3OH·$2CH_2Cl_2$·H_2O and

2a·$2CH_2Cl_2$ are hydrogen bonding and are described in Table S1 and the interactions are shown in Figure S5–Figure S7 in the Supporting Information.

Molecular structures of **1a**·CH_3OH·$2CH_2Cl_2$·H_2O and **2a**·$2CH_2Cl_2$ clearly authenticated that nitrosylation and the ligand nitration were two events that were common in both cases during our NO interaction studies.

The sites for nitration were different in the two cases; this occurs because the preferred *para* position (with respect to the phenolato function)[22] for nitration was blocked by the methyl group in complex **2a**. However, for complex **2a** the oxidative cyclization and formation of the benzoxazole derivative showed a rare type of reactivity of NO with this family of complexes (vide infra).

Spectroscopic Studies

Complexes **1** and **2** are red-brown in colour and the electronic spectra in dichloromethane are displayed in Figure S8. It has been found[3,10] that organometallic ruthenium complexes derived from type 1 ligands exhibit different colours from the change of substituents on the phenyl ring containing an aldehyde function. Complex **1** afforded two charge-transfer bands near 475 nm and 585 nm. On the other hand, the electronic spectrum of **2** gave rise to charge-transfer bands near 580 nm and 600 nm. These bands are probably a result of the ligand-to-metal charge transfer (LMCT) transition.[1–3,6] The electronic absorption spectra of complexes **1a** and **2a** (shown in Figure S9) exhibit one strong band near 312 nm along with a shoulder near 385 nm. These bands are probably from the charge-transfer transitions.[11]

The infrared spectra of all the complexes exhibit a band near 1590 cm^{-1} corresponding to the azomethine ($\nu_{C=N}$) stretching frequency, which is similar to the value reported by Chakravorty and coworkers.[3]

The presence of the $\{Ru–NO\}^6$ moiety[10,11] in both the nitrosyl complexes was also confirmed by the characteristic peaks in the infrared spectra. Complexes **1a** and **2a** have N–O stretching frequencies (ν_{NO}) near 1810 cm^{-1} and 1835 cm^{-1}, respectively. These values clearly indicate the presence of NO^+ bound to the Ru^{II} centre and a description of $\{Ru^{II}–NO^+\}^6$ for the $\{Ru–NO\}^6$ moiety present in **1a** and **2a** is proposed.[7] This is also supported by the data obtained from their crystal structures (vide supra). The peaks around 1090 cm^{-1} and 623 cm^{-1} show the presence of perchlorate ion in the complexes **1a** and **2a**, respectively. These complexes also afforded new bands in the range between 1290 and 1380 cm^{-1} and these bands are probably from the ring nitration (shown in the Supporting Information). In all the complexes, the peaks near 745 cm^{-1}, 695 cm^{-1} and 520 cm^{-1} show the presence of PPh_3 groups.[1,2,6,11]

The nitrosylation of the metal centre in the ruthenium cyclometalates **1a** and **2a** afforded clean NMR spectra that confirmed the diamagnetic behaviour of complexes with an $S = 0$ ground state. In the ^1H NMR spectrum of **1a** (shown in Figure S10), the peak at $\delta = 11.84$ ppm indicates the presence of a phenolic O–H proton. This peak disappeared after shaking the NMR sample solution in D_2O, which supported the presence of an exchangeable proton in the –OH functional group (Figure S14).[11,23] These data supported a dissociation of the $Ru–O_{Ph}$ bond during NO coordination in **1a**.

The ^1H NMR spectrum of **2a** clearly shows the presence of the methyl protons at ca. 2.5 ppm along with other protons present in the complex. Interestingly, no peak was found above 10.0 ppm, which indicates the absence of a phenolic O–H proton in complex **2a**. This data was consistent with our findings from structural calculations by X-ray crystallography and supported oxidative cyclization during the NO interaction. ^{31}P NMR spectra of the complexes **1a** and **2a** in CD_3CN indicate a single peak at about 20 ppm and ca. 18 ppm, respectively, confirming the *trans* disposition of the PPh_3 groups.[15,16]

Site Specific Orthometallation: A Reaction Model

The reaction of Schiff-base ligands with $Ru(PPh_3)_3Cl_2$ afforded organometallic ruthenium cyclometalates through orthometallation. Considering the orientation of the phenyl ring of *m*-nitrobenzaldehyde (Scheme 1, B), there are two possible sites for orthometallation. A crucial point for this reaction is that we ended up with a single product during the preparation of ruthenium cyclometalates and interestingly, after orthometallation the nitro group was found to be at a *para* position with respect to the Ru–C bond. It is reported in the literature that during orthometallation the metal centre could act as a nucleophile or an electrophile.[24–26] In the present study, the C–H bond activation seems to proceed by electrophilic attack on the aryl ring by the metal centre. The –I as well as –R effect of the $–NO_2$ group will decrease the electron density at the *ortho* and *para* positions, however, the effect at the *para* position will be lower compared to that at the *ortho* position. We speculate that the orthometallation occurred at the position *para* to the $–NO_2$ group, which had better electron density compared with the *ortho* position. Moreover, stability of the resultant complexes **1** and **2** may be obtained by keeping the $–NO_2$ group at the *para* position with respect to the Ru–C bond (vide infra).

Electrochemistry

The redox property of the metal centre was measured by cyclic voltammetry (Figure 3) in a dichloromethane solution using 0.1 M TBAP as the supporting electrolyte. Complex **1** exhibits quasi-reversible redox couples and $E_{1/2}$ values are found to be at –0.42 V and +0.80 V vs. Ag/AgCl. However, these two values for complex **2** are at –0.44 V and +0.72 V vs. Ag/AgCl [Figure 3 (a)]. The redox couples at the negative potential in **1** and **2** are assigned to the $Ru^{III}–Ru^{II}$ couple and those at the positive potential in both the complexes are described as a $Ru^{III}–Ru^{IV}$ couple.[1–4] The cyclic voltammetric data for the complexes are given in Table 2.

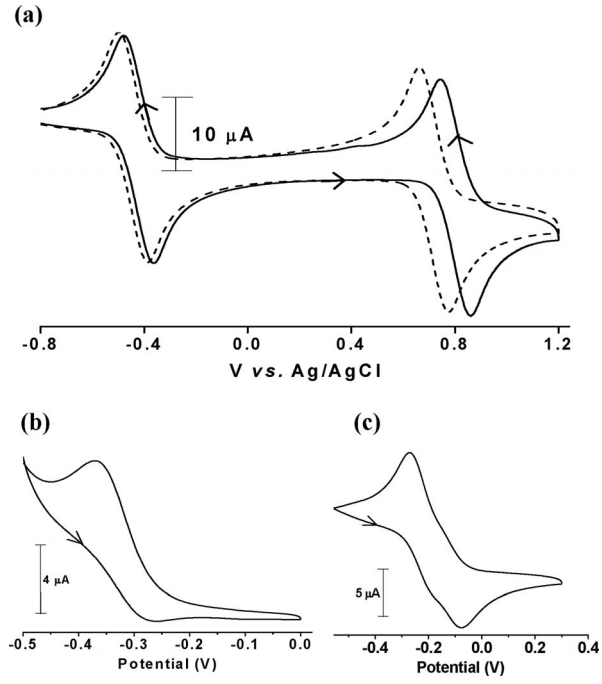

Figure 3. Cyclic voltammograms of 10^{-3} M solutions of (a) complex **1** (solid line) and complex **2** (dashed line). (b) Complex **1a** and (c) complex **2a** in dichloromethane, in the presence of 0.1 M tetrabutylammonium perchlorate (TBAP), using a working electrode (glassy-carbon), reference electrode (Ag/AgCl) and auxiliary electrode (platinum wire), scan rate = 0.1 V s^{-1}.

Table 2. Cyclic voltammetric data for complexes at 298 K. Conditions: solvent dichloromethane; supporting electrolyte TBAP (0.1 M); working electrode glassy carbon; reference electrode Ag/AgCl; scan rate 0.1 V s^{-1}; concentration 10^{-3} M.

Complex	$E_{1/2}$ [V][a] (ΔE_p [mV])[b]	
	Ru^{III}–Ru^{II}	Ru^{III}–Ru^{IV}
1	–0.42 (117)	+0.80 (118)
2	–0.44 (109)	+0.72 (114)
1a	–0.32 (102)	–
2a	–0.18 (190)	–

[a] $E_{1/2} = 0.5\ (E_{pa} + E_{pc})$ and [b] $\Delta E_p = (E_{pa} - E_{pc})$, where E_{pa} and E_{pc} are the anodic and cathodic peak potentials, respectively.

We have compared these $E_{1/2}$ values with the data reported by Chakravorty and coworkers (especially for complexes **5** and **5a** in that report).[3] A comparison of the $E_{1/2}$ values for the Ru^{III}–Ru^{II} redox couple clearly indicate better stabilization of the Ru^{II} in complexes **1** and **2**. It is imporant to note here that in this report because of orthometallation, the nitro group was situated *para* to the carbanion that was involved in Ru–C bond formation. On the other hand, in the above report[3] the nitro group was found to be at the *meta* position with respect to the carbanion. Hence, the presence of the $–NO_2$ group in the *para* position with respect to the Ru–C bond is probably responsible for the better stabilization of ruthenium(II) in this class of organometallic ruthenium cyclometalates.

In both the nitrosyl complexes **1a** and **2a**, quasi-reversible cyclic voltammograms are obtained [shown in Figure 3(b) and (c)] with $E_{1/2}$ values of –0.32 V and –0.18 V vs. Ag/AgCl, respectively. Hence in the nitrosyl complexes we found better stabilization of Ru^{II}. In the precursor complexes (**1** and **2**) we have determined the effect of the position of the nitro group on the phenyl ring, which was attached to the ruthenium centre through a σ-aryl Ru–C bond. This prompted us to examine the stabilization of ruthenium(II) in complexes **1a** and **2a** resulting from the change in position of the $–NO_2$ group in the ligand frame. A small decrease in the negative potential was obtained for complex **2a** compared with a similar complex reported recently.[10] After examination of electrochemical data of this report and our previous report,[10] we found that $E_{1/2}$ values for the Ru^{II}/Ru^{III} couple were near –0.20 V vs. Ag/AgCl for those complexes where oxidative cyclization has occurred. Other complexes, where we did not find the cyclization, afforded the same value in the range –0.30 V to –0.40 V vs. Ag/AgCl.

Photolysis Experiments of Nitrosyls

The photolability of coordinated NO of σ-aryl ruthenium nitrosyl complexes was examined in dichloromethane (for **1a**) and acetonitrile solutions (for **2a**). Solutions of the

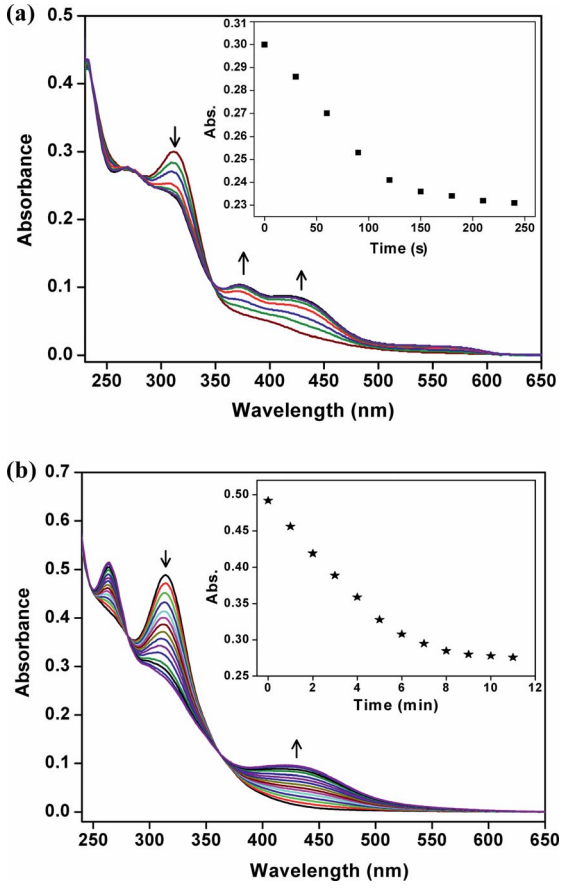

Figure 4. Photodissociation of (a) complex **1a** (ca. 1.1×10^{-5} M) in dichloromethane and (b) complex **2a** (ca. 1.8×10^{-5} M) in CH_3CN under illumination with a 100 W tungsten lamp. Repetitive scans were taken at 30 s intervals for **1a** and at 1 min intervals for **2a**. Inset: Time-dependent changes in absorbance at λ = 311 nm and λ = 314 nm for **1a** and **2a**, respectively.

complexes were stable in the dark, however, when these solutions were exposed to visible light (100 W tungsten lamp), a rapid change in colour from orange-yellow to red-brown was observed.

Spectral changes upon irradiation of a solution of **1a** (≈10^{-5} M) in dichloromethane with a 100 W tungsten lamp are shown in Figure 4(a) and the spectral changes give rise to three clear isosbestic points near 265 nm, 280 nm and 350 nm. Interestingly we observed that after the photolysis experiment of **1a**, the electronic absorption spectrum of the resulting solution was similar to the spectrum of **1**. This prompted us to characterize the resultant complex after the photocleavage reaction. The resultant complex was characterized by spectroscopic and electrochemical studies (shown in the Supporting Information, Figure S15). The data indicated the formation of ligand nitrated **1** (**1b**). This complex (**1b**) also reacts with nitric oxide and liberates NO under photolytic conditions (Scheme S1). Similar spectral changes were also observed with complex **2a** in an acetonitrile [shown in Figure 4(b)] solution. In this case, the isosbestic points are near 278 nm and 360 nm. A comparison of the data dispalyed in the inset clearly shows that in the presence of visible light, the release of NO in **2a** is slower than that for **1a**.

Transfer of NO to Myoglobin

The photocleavage of the coordinated NO was also confirmed by trapping the liberated NO by reduced myoglobin (shown in Figure S16). When an acetonitrile solution of complex **1a** was added to a buffer solution of reduced myoglobin under dark conditions no reaction was observed. However, when the same mixture was exposed to a tungsten lamp (100 W) for 2–3 min, its absorption spectrum at 420 nm showed the formation of a Mb–NO adduct.[11,27]

Determination of the Concentration of NO by Griess Reaction

The amount of NO released by the complexes **1a** and **2a**, synthesized in this report, was determined by using the Griess reagent.[28] We prepared the standard curve with different concentrations of $NaNO_2$ (5–50 μM) in solution (shown in Figure S18). From the molar extinction coefficient of dye (at 540 nm, ε = 41000 $M^{-1}cm^{-1}$)[29] the $NaNO_2$ standard curve predicted that the concentration of NO generated from an acidified nitrite solution was the concentration of $NaNO_2$ (±5 μM). The change in the absorbance of the dye (produced by the Griess reaction) in the dark as well as in the presence of light (UV and visible) clearly expressed the presence of photolabile NO in the nitrosyl complexes and this observation also supported our previous experiments, namely electronic absorption spectral studies (Figure 4) and trapping of NO by reduced myoglobin (Figure S16). The generation of a peak near 538 nm clearly indicates the formation of NO in solution. Hence, we could predict that photolabile coordinated NO was responsible for the change in absorbance at the same wavelength. It is important to mention here that in the dark we observed little change in absorbance at 538 nm, which indicated the loss of NO from **1a** and **2a**. The loss of NO was found to be ca. 1.5% with respect to the concentration of the complexes (50 μM) in solution. Using 50 μM of both of the complexes **1a** and **2a**, we found that in the dark the concentration of

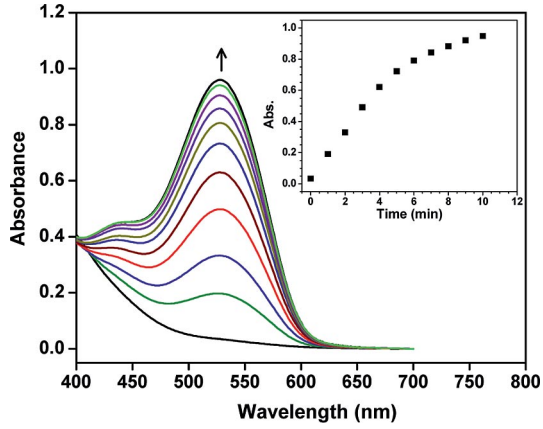

Figure 5. Electronic spectra of the formation of dye when the Griess reagent (100 μL) was treated with complex **1a** (50 μM) in the presence of light (100 W tungsten lamp). Repetitive scans were taken at 1 min intervals. Inset: Time-dependent change in absorbance at λ = 538 nm.

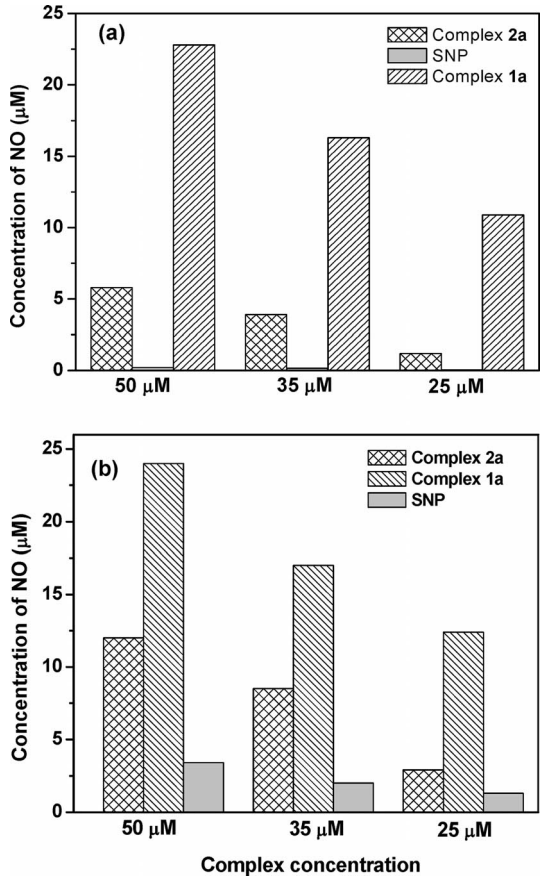

Figure 6. Bar diagrams showing the amount of photoreleased NO (dye formation) from the complexes under exposure to (a) visible light and (b) UV light for 15 min.

produced dye was ca. 0.8 μM. Shining of visible light (100 W tungsten lamp) onto the 50 μM solution of **1a** for 10–15 min gave rise to the formation of about 23.0 μM of dye (Figure 5), however, the solution of **2a** with the same concentration produced only ca. 6 μM of azo dye in visible light [Figure 6(a), Table 3]. We have compared our data with the data obtained from sodium nitroprusside (SNP), a donor of nitric oxide.[12] In visible light [Figure 6 (a), Table 3], a 50 μM solution of sodium nitroprusside produced a very small amount of nitric oxide (ca. 0.2 μM in 15 min), however, in ultravoilet light [Figure 6 (b), Table 3], the same solution provided about 4.0 μM of nitric oxide.

Table 3. Determination of the amount of dye produced from the complexes **1a**, **2a** and sodium nitroprusside (SNP) on reaction with the Griess reagent in the dark, visible light and UV light.

Complex	Complex conc. [μM]	Concentration of dye produced [μM][a]		
		In the dark	Exposure to visible light	Exposure to UV light
1a	50	0.73	23.00	24.0
2a	50	0.84	5.74	12.0
SNP	50	0.04	0.22	3.4

[a] Average of three experiments.

These data afforded the formation of NO in solution and the concentration of photoreleased NO in complexes **1a** and **2a** was found to be greater in comparison with the NO released by SNP.

The quantum yield (ϕ) values for complexes **1a** and **2a** (λ_{irr} = 365 nm) were found to be 0.017 ± 0.001 and 0.012 ± 0.001, respectively, in acetonitrile solutions. These data showed a slightly higher NO donor capacity for **1a** than for **2a**.

Role of the $-NO_2$ Group in Oxidative Cyclization and NO Delivery

It is important to note here that in this study of NO reactivity we have found oxidative cyclization and concomitant formation of the substituted 2-phenylbenzoxazole derivative, only when a methyl group was present in the position *trans* to the phenolato function [described in Scheme 4 (A)]. We have compared these results with our previous observations.[10] Moreover, to better understand the findings, we studied the synthesis of another ruthenium nitrosyl complex **3s** (described in the Supporting Information, Scheme S2) in order to observe the positional effect of the $-NO_2$ group. The following points are important in this regard: First, the ^{1}H NMR spectrum of **3s** (Figure S22) did not afford the characteristic peak for the –OH function. Second, electrochemical data for **3s** (Figure S23) afforded the $E_{1/2}$ redox couple for Ru^{II}/Ru^{III} at –0.21 V vs. Ag/AgCl. Third, UV/Vis spectroscopic data (Figure S24) for the photocleavage experiment of NO in **3s** resembles that of **4s** (complex **2** of ref.[10]). Four, the amount of liberated NO from **3s** and **4s** was similar to that of **2a** (Table S2, Figure S25 and S26). All these data clearly indicate that the presence of the methyl group on the ring containing the phenolato function was not necessary for the cyclization reaction for the complexes obtained from *p*-nitrobenzaldehyde [described in Scheme 4 (B)].

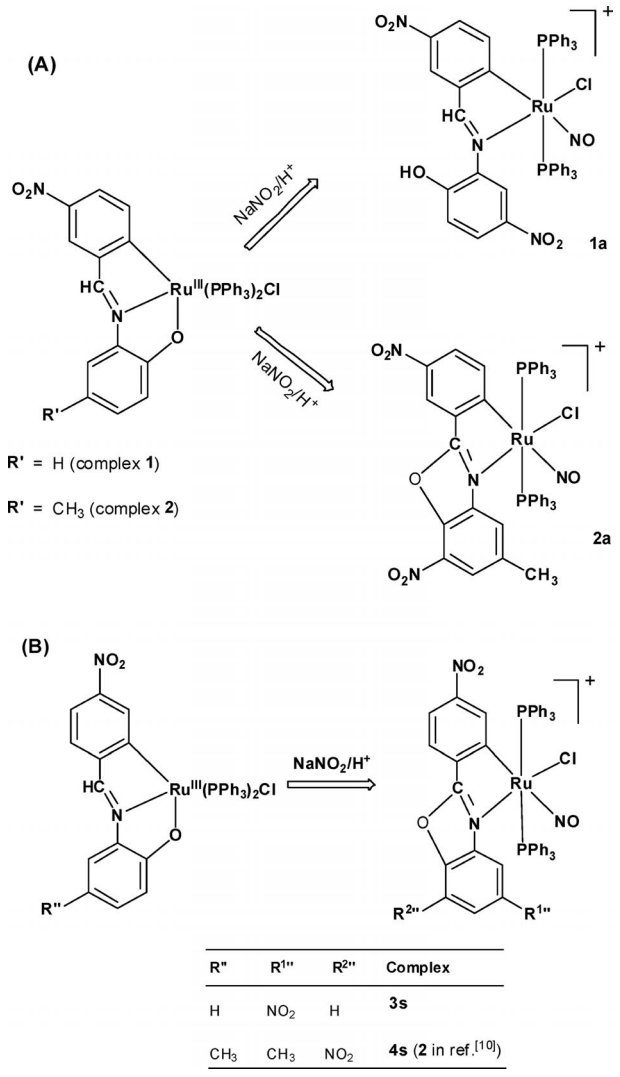

R"	R1"	R2"	Complex
H	NO_2	H	**3s**
CH_3	CH_3	NO_2	**4s** (**2** in ref.[10])

Scheme 4.

Conclusions

The following are the principle findings of the present study. The organometallic ruthenium(III) cyclometalates **1** and **2** were synthesized by site-specific orthometallation. In these complexes, the metal–carbon bond was established in such a way that the electron-withdrawing $-NO_2$ group was found to be at the *para* position with respect to the Ru–C bond. The interaction of nitric oxide with these complexes was investigated and complexes **1a** and **2a** were obtained from **1** and **2**, respectively. The *trans* effect of carbanion gave rise to dissociation of the phenolato function and NO was coordinated to the metal centre. Molecular structures of **1a**·CH_3OH·$2CH_2Cl_2$·H_2O and **2a**·$2CH_2Cl_2$ were determined by X-ray crystallography. Interestingly, structure determination clearly authenticated three important events of

the NO rectivity studies. First, nitrosylation of the metal centre and synthesis of the ruthenium nitrosyl complexes. Second, ligand nitration was observed in both nitrosyl complexes. Third, oxidative cyclization and formation of the benoxazole ring in **2a**.

Photolability of NO was authenticated by UV/Vis spectral studies and trapping experiments. In **1a**, the ruthenium–phenolato bond was reestablished after the photorelease of coordinated NO. The Ru–N–O angle and N–O bond distances clearly indicated the presence of a $\{Ru^{II}NO^{+}\}^{6}$ moiety in both the nitrosyl complexes. Both **1a** and **2a** exhibited ^{1}H NMR as well as ^{31}P NMR spectra. These findings were supported by the diamagnetic behaviour of **1a** and **2a** and NO stretching frequencies in the IR spectral studies. An electrochemical investigation indicated Ru^{II}–Ru^{III} and Ru^{III}–Ru^{IV} redox couples for **1** and **2**. On the other hand, only a Ru^{II}–Ru^{III} couple was obtained for complexes **1a** and **2a**.

We found that the methyl group was necessary on the ring containing the phenolato function for oxidative cyclization in the complexes described in this report. However, for the ruthenium cyclometalates obtained from *p*-nitrobenzaldehyde[10] the presence of a methyl group was not important.

We have estimated the amount of available NO in solution during these photolytic reactions and we compared our data with the same obtained from sodium nitroprusside. It has been found that complex **1a** was equally efficient in NO delivery in visible and UV light and that the amount of NO produced by **1a** was higher than that of **2a**. Complexes **3s** and **4s** were similar to **2a** in terms of NO generation in solution. Ruthenium cyclometalates have never been used for photoinduced delivery of nitric oxide[30] and complexes described in this report demand their application in photodynamic therapy.

A study of the effect of the electron-donating group of the phenyl ring containing an aldehyde function in the coordination and photolability of NO is under progress. Biological applications of these complexes along with the synthesis of substituted benzoxazole are also being investigated.

Experimental Section

Materials: All the solvents used were of reagent grade. The analytical grade reagents; sodium nitrite, (Sigma Aldrich, Steinheim, Germany), $RuCl_3 \cdot 3H_2O$, triphenylphosphane (SRL, Mumbai, India), 2-aminophenol, 2-amino-4-methylphenol, 3-nitrobenzaldehyde, sodium perchlorate monohydrate, sulfanilamide, naphthylethylenediamine dihydrochloride (NED) (Himedia Laboratories Pvt. Ltd., Mumbai, India), disodium hydrogen phosphate anhydrous (RFCL Ltd. New Delhi, India) and sodium dihydrogen phosphate (Chemport India Pvt. Ltd. Mumbai, India) were used as obtained. Double-distilled water was used in all of the experiments. Equine skeletal muscle myoglobin was obtained from Sigma Aldrich, Steinheim, Germany.

Physical Measurements: Electronic absorption spectra of all the complexes were recorded in dichloromethane and acetonitrile solvents with an Evolution 600, Thermo Scientific UV/Vis spectrophotometer. Infrared spectra were obtained as KBr pellets with a Thermo Nicolet Nexus FTIR spectrometer, using 16 scans and were reported in cm^{-1}. ^{1}H and ^{31}P NMR spectra were recorded with a Bruker AVANCE, 500.13 MHz spectrometer in the deuterated solvents. Cyclic voltammetric studies were performed with a CH-600 electroanalyser in dichloromethane with 0.1 M tetrabutylammonium perchlorate (TBAP) as the supporting electrolyte. The working electrode, reference electrode and auxiliary electrode were glassy carbon electrode, Ag/AgCl electrode and Pt wire, respectively. The concentration of the compounds was in the order of 10^{-3} M. The ferrocene/ferrocenium couple occurred at $E_{1/2}$ = +0.51 (102) V vs. Ag/AgCl (scan rate 0.1 $V s^{-1}$) in dichloromethane under the same experimental conditions. Quantum yields were determined by actinometry studies using a ferric oxalate solution. The intensity of the light (λ_{irr} = 365 nm) was determined using a ferrioxalate actinometer (0.006 M solution of potassium ferrioxalate in 0.1 N H_2SO_4).[31–33] Quantum yields (ϕ) of the NO photorelease for complexes **1a** and **2a** were determined from the decrease in their absorption bands near 310 nm and 314 nm when irradiated with 365 nm light and were calculated by following the procedure reported earlier.[7,33,34]

Preparation of Complexes

Caution: Perchlorate salts of metal complexes with organic ligands are potentially explosive. Only a small amount of material should be prepared and handled carefully.

Synthesis of Ligands: The Schiff base ligands $L^{SB1}H_2$ [2-(3-nitrobenzylideneamino)phenol] and $L^{SB2}H_2$ [4-methyl-2-(3-nitrobenzylideneamino)phenol] were synthesized by the condensation of 3-nitrobenzaldehyde with 2-aminophenol and 2-amino-4-methylphenol, respectively, in ethanol by following the procedure reported by Chakravorty and his coworkers.[3]

The precursor complex $[Ru(PPh_3)_3Cl_2]$ was prepared by the procedure reported earlier.[35]

$[Ru(L^{SB1})(PPh_3)_2Cl]$ (1): A batch of $L^{SB1}H_2$ (0.036 g, 0.15 mmol) and ethanol (5 mL) was added to a warm solution of $Ru(PPh_3)_3Cl_2$ (0.096 g, 0.10 mmol) in ethanol (30 mL). The mixture was heated under reflux for 2 h and was then allowed to cool to obtain a precipitate of a red-brown colour. The solid was filtered out and was washed thoroughly with ethanol and diethyl ether and was then dried. Complex **1** (0.062 g, 0.069 mmol) was eluted on an alumina column by a dichloromethane/hexane (1:1) mixture; yield 69%. IR (KBr disk): $\tilde{\nu}$ = 1580 ($\nu_{C=N}$), 1482, 1434, 1332, 1310 (ν_{NO2}), 1284, 742, 695, 515 (ν_{PPh3}) cm^{-1}. UV/Vis (CH_2Cl_2): λ_{max} (ε, $M^{-1}cm^{-1}$) = 267 (38182), 371 (13636), 475 (5636), 585 (2273) nm.

$[Ru(L^{SB2})(PPh_3)_2Cl]$ (2): This was prepared by the same procedure as that used for **1**, with $Ru(PPh_3)_3Cl_2$ (0.096 g, 0.10 mmol) and $L^{SB2}H_2$ (0.038 g, 0.15 mmol); yield 63%. IR (KBr disk): $\tilde{\nu}$ = 1595 ($\nu_{C=N}$), 1570, 1482, 1433, 1330, 1309 (ν_{NO2}), 1298, 1266, 740, 693, 519 (ν_{PPh3}) cm^{-1}. UV/Vis (CH_2Cl_2): λ_{max} (ε, $M^{-1}cm^{-1}$) = 270 (39231), 376 (12308), 580 (5385), 598 (2308) nm.

$[Ru(L^{SB3}H)(PPh_3)_2(NO)Cl]ClO_4$ (1a): [where $L^{SB3}H_2$ = 4-nitro-2-(3-nitrobenzylideneamino)phenol]: A batch of complex **1** (0.016 g, 0.018 mmol) was dissolved in dichloromethane (25 mL) to obtain a brownish-red coloured solution in a round-bottomed flask (100 mL). Acidified distilled water (20 mL) was then layered over this solution. Sodium nitrite (0.19 g, 2.7 mmol) was added to the bilayer solution and the mixture was stirred at room temperature for 1 h to obtain a yellowish-orange coloured solution of complex **1a**. A dichloromethane layer was separated out and $NaClO_4$ (in excess) with methanol (5 mL) was added to this solution. Stirring

of this solution was continued for another 1 h. A yellowish-orange solid was precipitated out by the evaporation of the solvent. In order to remove the excess $NaClO_4$, the compound was further dissolved in dichloromethane and was filtered off. Complex **1a** (0.012 g, 0.011 mmol) was eluted on an alumina column by a dichloromethane/methanol (9:1) mixture. Single crystals of the complex for X-ray crystallography were obtained within 2 d upon slow evaporation of a dichloromethane/methanol mixture; yield 61.11%. IR (KBr disk): $\tilde{\nu}$ = 1811 (ν_{NO}), 1590 ($\nu_{C=N}$), 1480, 1434, 1345, 1304 (ν_{NO2}), 1089, 623 (ν_{ClO4}), 748, 693, 518 (ν_{PPh3}) cm^{-1}. UV/Vis (CH_2Cl_2): λ_{max} (ε, $M^{-1}cm^{-1}$) = 385 (5273), 311 (27455) nm. ^{31}P NMR (CD_3CN, 500 MHz): δ = 20.35 ppm. ^1H NMR [$(CD_3)_2SO$, 500 MHz]: δ = 11.84 (s, 1 H), 8.83 (s, 1 H), 8.47 (s, 1 H), 8.06 (d, 1 H), 7.46–7.21 (m, 31 H), 6.97 (s, 1 H), 6.95 (d, 1 H) and 6.84 (d, 1 H) ppm.

[Ru(L^{BOX})(PPh$_3$)$_2$(NO)Cl]ClO$_4$ (2a): {where L^{BOX}H = 5-methyl-7-nitro-2-(3-nitrophenyl)benzoxazole}: Complex **2a** was prepared by the same procedure as that used for **1a**. Single crystals of the complex **2a** for X-ray crystallography were obtained within 3 d in the dark upon slow evaporation of a dichloromethane/methanol mixture; yield 59%. IR (KBr disk): $\tilde{\nu}$ = 1837 (ν_{NO}), 1590, 1380, 1350, 1233, 1091, 623 (ν_{ClO4}), 750, 695, 517 (ν_{PPh3}) cm^{-1}. UV/Vis (CH_3CN): λ_{max} (ε, $M^{-1}cm^{-1}$) = 384 (6722), 314 (26667) nm. ^{31}P NMR (CD_3CN, 500 MHz): δ = 18.12 ppm. ^1H NMR [$(CD_3)_2SO$, 500 MHz]: δ = 8.49 (d, 1 H), 8.15 (s, 1 H), 7.69 (d, 1 H), 7.37–7.25 (m, 32 H), and 2.45 (s, 3 H) ppm.

Transfer of NO to Myoglobin

Preparation of the Phosphate Buffer Solution: A phosphate buffer solution (50 mM) of pH 6.8 was prepared by adding $NaH_2PO_4{\cdot}2H_2O$ (0.4192 g) and anhydrous Na_2HPO_4 (0.3283 g) to MilliQ water (50 mL) and making the volume to 100 mL in a volumetric flask.

Preparation of the Myoglobin Stock Solution: Equine skeletal muscle myoglobin (5 mg) was dissolved in the above prepared buffer solution (5 mL).

Binding of the Photoreleased NO with Myoglobin: Electronic absorption spectra were obtained against the phosphate buffer as reference. A myoglobin stock solution (100 μL) was diluted up to 1000 μL in a quartz cuvette with an optical length of 1 cm and sealed with a rubber septum. Its UV/Vis spectrum showed an intense band at 409 nm (Soret band). The UV/Vis spectrum of reduced myoglobin at 433 nm was obtained by the addition of excess sodium dithionite to the same cuvette. When complex **1a** was added to the buffer solution of reduced myoglobin under dark conditions, no reaction was observed. However, when the same mixture was exposed to a tungsten lamp (100 W) for 2 min, its absorption spectrum at 420 nm showed the formation of a Mb–NO adduct.[11,27]

Estimation of NO Production by the Griess Reaction: The production of NO by complexes **1a** and **2a** was estimated using the Griess reagent (GR).[28] It was prepared fresh by mixing equal volumes of 1% sulfanilamide in 5% orthophosphoric acid and 0.1% naphthylethylene diamine dihydrochloride (NED) in water. To estimate the production of NO or NO_2, the absorbance was measured at 538 nm to determine the formation of azo dye. Aqueous solutions of sodium nitrite with different concentrations (5–50 μM) were used to prepare standard curves for the determination of nitrite.

X-ray Crystallography: Orange-red crystals of **1a**·$CH_3OH{\cdot}2CH_2Cl_2{\cdot}H_2O$ and **2a**·$2CH_2Cl_2$ were obtained by slow evaporation of solution of the complexes in a CH_2Cl_2/methanol mixture. The crystal structures showed the presence of water molecules in the lattice. The X-ray data collection and processing for complexes were performed with a Bruker Kappa Apex-II CCD diffractometer by using graphite-monochromated Mo-K_α radiation (λ = 0.71073 Å) at 273 K for **1a**·$CH_3OH{\cdot}2CH_2Cl_2{\cdot}H_2O$ and at 296 K for **2a**·$2CH_2Cl_2$ (Table 4). Crystal structures were solved by direct methods. Structure solutions, refinement and data output were carried out with the SHELXTL program.[36,37] All non-hydrogen atoms were refined anisotropically. Hydrogen atoms were placed in geometrically calculated positions and refined using a riding model. Images were created with the DIAMOND program.[38]

Table 4. Crystal data and structural refinement parameters for complexes **1a**·$CH_3OH{\cdot}2CH_2Cl_2{\cdot}H_2O$ and **2a**·$2CH_2Cl_2$.

	1a·$CH_3OH{\cdot}2CH_2Cl_2{\cdot}H_2O$	**2a**·$2CH_2Cl_2$
Empirical formula	$C_{52}H_{48}Cl_6N_4O_{14}P_2Ru$	$C_{52}H_{42}Cl_6N_4O_{10}P_2Ru$
M_r [g mol^{-1}]	1328.65	1258.61
Temperature [K]	273(2)	296(2)
λ [Å] (Mo-K_α)	0.71073	0.71073
Crystal system	triclinic	monoclinic
Space group	$P\bar{1}$	$P2_1/n$
a [Å]	12.505(3)	13.4992(4)
b [Å]	13.488(3)	23.2857(7)
c [Å]	18.220(4)	17.6737(5)
α [°]	93.11(3)	90
γ [°]	101.47(3)	90
β [°]	106.87(3)	101.980(10)
V [Å^3]	2861.5(13)	5434.5(3)
Z	2	4
$\rho_{calcd.}$ [g cm^{-3}]	1.542	1.538
$F(000)$	1352.0	2552.0
Theta range [°]	1.18–25.00	1.47–28.35
Index ranges	$-14 < h < 14$, $-16 < k < 16$, $-21 < l < 21$	$-18 < h < 18$, $-31 < k < 31$, $-23 < l < 23$
Data / restraints / parameters	10077 / 0 / 719	13337 / 0 / 677
GOF[a] on F^2	1.190	1.317
R_1[b] [$I > 2\sigma(I)$]	0.0595	0.0636
R_1 [all data]	0.1394	0.1143
wR_2[c] [$I > 2\sigma(I)$]	0.1574	0.1802
wR_2 [all data]	0.2141	0.2155

[a] GOF = $\{\Sigma[w(F_o^2 - F_c^2)^2]/M - N\}^{1/2}$ (M = number of reflections, N = number of parameters refined). [b] $R_1 = \sigma||F_o| - |F_c||/\Sigma|F_o|$. [c] $wR_2 = \{\Sigma[w(F_o^2 - F_c^2)^2]/\Sigma[w(F_o^2)^2]\}^{1/2}$.

Supporting Information (see footnote on the first page of this article): Characterization of complexes by IR, UV/Vis and NMR spectral studies. The standard curve of $NaNO_2$ for the Griess reaction. X-ray crystallographic data of complexes **1a**·$CH_3OH{\cdot}2CH_2Cl_2{\cdot}H_2O$ and **2a**·$2CH_2Cl_2$ in CIF format.

Acknowledgments

K. G. is thankful to the Council of Scientific and Industrial Research (CSIR), New Delhi for financial assistance [01(2229)/08/EMR-II, dated 06 March, 2008]. S. K. and R. K. are thankful to the CSIR for financial assistance. U. P. S. is thankful for support by single-crystal X-ray facility of the IIT Roorkee.

[1] R. Raveendran, S. Pal, *J. Organomet. Chem.* **2009**, *694*, 1482–1486.
[2] P. Munshi, R. Samanta, G. K. Lahiri, *J. Organomet. Chem.* **1999**, *586*, 176–183.
[3] P. Ghosh, A. Pramanik, N. Bag, G. K. Lahiri, A. Chakravorty, *J. Organomet. Chem.* **1993**, *454*, 237–241.

[4] G. K. Lahiri, S. Bhattacharya, M. Mukherjee, A. K. Mukherjee, A. Chakravorty, *Inorg. Chem.* **1987**, *26*, 3359–3365.
[5] H. Hadadzadeh, M. C. DeRosa, G. P. A. Yap, A. R. Rezvani, R. J. Crutchley, *Inorg. Chem.* **2002**, *41*, 6521–6526.
[6] S. Kannan, R. Ramesh, Y. Liu, *J. Organomet. Chem.* **2007**, *692*, 3380–3391.
[7] M. J. Rose, P. K. Mascharak, *Coord. Chem. Rev.* **2008**, *252*, 2093–2114.
[8] P. C. Ford, J. Bourassa, K. Miranda, B. Lee, I. Lorkovic, S. Boggs, S. Kudo, L. Laverman, *Coord. Chem. Rev.* **1998**, *171*, 185–202.
[9] M. G. Sauaia, R. G. de Lima, A. C. Tedesco, R. S. da Silva, *J. Am. Chem. Soc.* **2003**, *125*, 14718–14719.
[10] K. Ghosh, S. Kumar, R. Kumar, U. P. Singh, N. Goel, *Inorg. Chem.* **2010**, *49*, 7235–7237.
[11] K. Ghosh, S. Kumar, R. Kumar, U. P. Singh, N. Goel, *Organometallics* **2011**, *30*, 2498–2505.
[12] C. Xin Zhang, S. J. Lippard, *Curr. Opin. Chem. Biol.* **2003**, *7*, 481–489.
[13] M. J. Rose, P. K. Mascharak, *Curr. Opin. Chem. Biol.* **2008**, *12*, 238–244.
[14] R. K. Afshar, A. K. Patra, M. M. Olmstead, P. K. Mascharak, *Inorg. Chem.* **2004**, *43*, 5736–5743.
[15] B. P. Sullivan, J. M. Calvert, T. J. Meyer, *Inorg. Chem.* **1980**, *19*, 1404–1407.
[16] K. Ghosh, S. Kumar, R. Kumar, *Inorg. Chem. Commun.* **2011**, *14*, 146–149.
[17] M. J. Rose, A. K. Patra, E. A. Alcid, M. M. Olmstead, P. K. Mascharak, *Inorg. Chem.* **2007**, *46*, 2328–2338.
[18] M. J. Rose, M. M. Olmstead, P. K. Mascharak, *J. Am. Chem. Soc.* **2007**, *129*, 5342–5343.
[19] N. Chanda, D. Paul, S. Kar, S. M. Mobin, A. Datta, V. G. Puranik, K. K. Rao, G. K. Lahiri, *Inorg. Chem.* **2005**, *44*, 3499–3511.
[20] J. H. Enemark, R. D. Feltham, *Coord. Chem. Rev.* **1974**, *13*, 339–406.
[21] G. R. Desiraju, T. Steiner, *The Weak Hydrogen Bond in Structural Chemistry and Biology*, Oxford University Press, New York, **1999**.
[22] B. Birkmann, B. T. Owens, S. Bandyopadhyay, G. Wu, P. C. Ford, *J. Inorg. Biochem.* **2009**, *103*, 237–242.
[23] K. Ghosh, S. Pattanayak, A. Chakravorty, *Organometallics* **1998**, *17*, 1956–1960.
[24] N. Chitrapriya, V. Mahalingam, M. Zeller, K. Natarajan, *Polyhedron* **2008**, *27*, 1573–1580.
[25] R. L. Brainard, W. R. Nutt, T. R. Lee, G. M. Whitesides, *Organometallics* **1988**, *7*, 2379–2386.
[26] R. Cordone, W. D. Harman, H. Taube, *J. Am. Chem. Soc.* **1989**, *111*, 2896–2900.
[27] S. Maji, B. Sarkar, M. Patra, A. K. Das, S. M. Mobin, W. Kaim, G. K. Lahiri, *Inorg. Chem.* **2008**, *47*, 3218–3227.
[28] A. Chakraborty, N. Gupta, K. Ghosh, P. Roy, *Toxicol. in vitro* **2010**, *24*, 1215–1228.
[29] D. Tsikas, *J. Chromatogr. B* **2007**, *851*, 51–70.
[30] J. P. Djukic, J. B. Sortais, L. Barloy, M. Pfeffer, *Eur. J. Inorg. Chem.* **2009**, 817–853.
[31] H. J. Kuhn, S. E. Braslavsky, R. Schmidt, *Pure Appl. Chem.* **1989**, *61*, 187–210.
[32] S. K. Nayak, G. J. Farrell, T. J. Burkey, *Inorg. Chem.* **1994**, *33*, 2236–2242.
[33] C. F. Works, C. J. Jocher, G. D. Bart, X. Bu, P. C. Ford, *Inorg. Chem.* **2002**, *41*, 3728–3739.
[34] A. K. M. Holanda, F. O. N. da Silva, J. R. Sousa, I. C. N. Diogenes, I. M. M. Carvalho, I. S. Moreira, M. J. Clarke, L. G. F. Lopes, *Inorg. Chim. Acta* **2008**, *361*, 2929–2933.
[35] T. A. Stephenson, G. Wilkinson, *J. Inorg. Nucl. Chem.* **1966**, *28*, 945–956.
[36] G. M. Sheldrick, *Acta Crystallogr., Sect. A* **1990**, *46*, 467–473.
[37] G. M. Sheldrick, *SHELXTL–NT 2000*, version 6.12, Reference Manual, University of Göttingen, Pergamon, New York, **1980**.
[38] B. Klaus, University of Bonn, Germany, *DIAMOND*, version 1.2c, **1999**.

Received: September 27, 2011
Published Online: January 23, 2012

